Journal of Magnetism and Magnetic Materials 474 (2019) 400–405

Contents lists available at ScienceDirect

Journal of Magnetism and Magnetic Materials

journal homepage: www.elsevier.com/locate/jmmm

Research articles

Magneto-ultrasonic heating with nanoparticles

K. Kaczmarek[a,*], T. Hornowski[a], I. Antal[b], M. Timko[b], A. Józefczak[a,*]

[a] Institute of Acoustics, Faculty of Physics, Adam Mickiewicz University, Umultowska 85, Poznań 61-614, Poland
[b] Institute of Experimental Physics, Slovak Academy of Sciences, Watsonova 47, Košice 040 01, Slovakia

ARTICLE INFO

Keywords:
Sonomagnetic heating
Focused ultrasound hyperthermia
Magnetic hyperthermia
Sonosensitizers

ABSTRACT

Recently, there has been a great interest in the application of multimodal hyperthermia. Hyperthermia, a controlled increase of temperature in tissues up to 42–45 °C, is a very promising anti-cancer medical treatment. Hyperthermia can be induced by means of ultrasound wave, alternating magnetic field, radiowave, laser light, etc. In our research, we combine magnetic hyperthermia with ultrasound thermal treatment to facilitate a more efficient, innovative sonomagnetic therapy. The experiments are performed using ultrasound phantoms doped with magnetic nanoparticles. These nanoparticles act like sonosensitizers and become the source of supplementary ultrasound attenuation which consequently leads to the increase of temperature. Because of their sensitivity to magnetic field they are also the source of heat in magnetic hyperthermia. In order to investigate the thermal effect of multimodal hyperthermia, phantoms are simultaneously irradiated with a focused ultrasound beam and exposed to the AC magnetic field. We demonstrate that this double thermal stimulation of phantoms doped with nanoparticles provides better heating efficiency which enables more precise control over the heating process. Magneto-ultrasonic heating creates more effective hyperthermia and has a big application potential in treating cancer at a lower magnetic particle concentration. The coupling of magnetic and ultrasonic hyperthermia gives the possibility for developing the new, innovative sonomagnetic thermal therapy.

1. Introduction

The new methods of cancer treatment are constantly being sought. Recently, there has been a great interest in the application of multimodal thermal treatments. The efforts are focused on improving and modifying the existing thermal procedures by combining them with other methods. Such combinations are called bimodal or multimodal therapies. Over the past years much effort has been put in combining chemotherapy with photo-thermal therapy [1,2], magnetic hyperthermia with photo-thermal treatment [3], chemotherapy with nanoparticle drug delivery [4,5], and high-intensity focused ultrasound (HIFU) with nanomedicine [6,7]. Moreover, hyperthermia has been also used as a combination therapy to enhance efficacy of chemotherapy by improving the delivery of targeted nanomedicines [8]. Thermal effects of ultrasound can also be applied for triggered drug release. In order to avoid unintended damage of surrounding cells during prolonged heating, drug carriers are designed to release their payload at the temperature (e.g., 42–43 °C) a few degrees above the physiological temperature [9]. The application of such a combined therapies has many advantages. It allows us to reduce the amount of, potentially toxic in high concentrations, nanoparticles, drugs, substances, etc. used in the therapy [3]. The combined therapies can lead to achieve of the desired temperature increase in a shorter time, which can reduce negative side effects of treatment like discomfort, skin burns, pain [10,11]. Moreover, combination of few different therapies allow us also to decrease the values of such parameters as power, intensity, irradiation time of each method.

Recently, there is also a lot of interest in the use of materials such as iron oxide nanoparticles, which have capacity to act as agent in many therapies: magnetic hyperthermia, thermo-ablation, photo-thermal treatment, magnetic resonance imaging (MRI) [3,12–14]. Our previous experimental results and theoretical modeling show that magnetic nanoparticles are also good candidates for sonosensitizing materials in the case of ultrasound-induced hyperthermia. Their presence in tissue-mimicking phantoms increases the ultrasonic attenuation with a consequent temperature rise, reducing the wave intensity and the exposure time required to obtain bioeffects [15]. Magnetic nanoparticles can also be used as nanocarriers for different therapeutic agents, thus effectively combine various cancer treatment methods [12]. Superparamagnetic iron oxide nanoparticles (SPION) are also used for selective induction of heat by an externally applied AC magnetic field [16,17]. This method is called magnetic hyperthermia. Because nanoparticles have the dual ability to act as both magnetic and sonosensitizer agents, magnetic and ultrasonic hyperthermia may work synergistically to produce a more

* Corresponding authors.
E-mail addresses: katarzyna.kaczmarek@amu.edu.pl (K. Kaczmarek), aras@amu.edu.pl (A. Józefczak).

https://doi.org/10.1016/j.jmmm.2018.11.062
Received 20 June 2018; Received in revised form 8 November 2018; Accepted 8 November 2018
Available online 09 November 2018
0304-8853/

efficient treatment [18]. This sonomagnetic therapy is a promising new technique. The basis of this novel therapy is to administer a very small amount of sonosensitizer, which can be activated by the simultaneous application of both the ultrasound and the magnetic field. This bimodal interaction will produce more heat in tumors.

In this study we have focused on evaluating the influence of magneto-ultrasonic heating on phantom temperature in the presence of SPION. The experiments are performed using tissue mimicking phantoms doped with magnetic nanoparticles. These nanoparticles become the source of supplementary ultrasound attenuation and also they are a source of heat in the magnetic hyperthermia. The combined treatment using a simultaneous application of the focused ultrasound wave and the AC magnetic field (bimodal sonomagnetic hyperthermia) leads to a higher temperature increase, which enables more precise control over the heating process. Magneto-ultrasonic heating creates very innovative, promising approach which has an application potential to treat cancer at lower SPION concentration.

2. Materials and methods

2.1. Preparation and characterization of $HClO_4$-stabilized SPION and their modification with glycine

In this research we used the magnetic nanoparticles dispersed in a fluid, a suspension that is called magnetic fluid (MF). Iron oxide nanoparticles were prepared by the coprecipitation of ferric and ferrous salts (molar ratio 2:1) in the base solution of 25% NH_4OH under constant stirring. The suspension was washed 4 times with water to reach an approximate pH of 7 [19,20]. After washing, concentrated $HClO_4$ was added to the precipitate and the outcome MF was centrifuged at 35,000 rpm for 60 min [21,22]. The SPION concentration in the MF was 50 mg/mL. Glycine was dissolved in ultrapure water and was added to MF in the ratio glycine/magnetic nanoparticles = 5. The mixture was stirred for 72 h at 25 °C. The SPION concentration in the sample magnetic nanoparticles modified with glycine was 34 mg/mL. Glycine was chosen as it is a chain amino acid easily adsorbed onto the iron oxide surface. Moreover nanoparticles covered with glycine show good colloidal stability and cytocompatibility with cell lines [23,24].

Magnetic properties which are very important to the aim of the study were investigated using a vibrating-sample magnetometer (VSM) installed on a cryogen-free superconducting magnet from Cryogenic Ltd. Fig. 1 presents the magnetic properties of the prepared magnetic fluid. It shows a narrow hysteresis loop for 298 K, which proves the

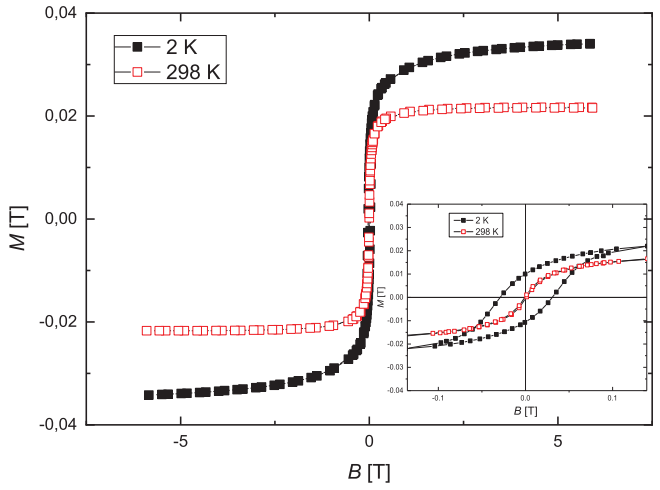

Fig. 1. Hysteresis loop obtained for 2 K and 298 K (the inset shows the zoom of the hysteresis loop in the range between −0.1 and 0.1 T). Squares denote the experimental data whereas solid line shows the sum of Langevin functions for different particle diameters weighted by the particles size distribution.

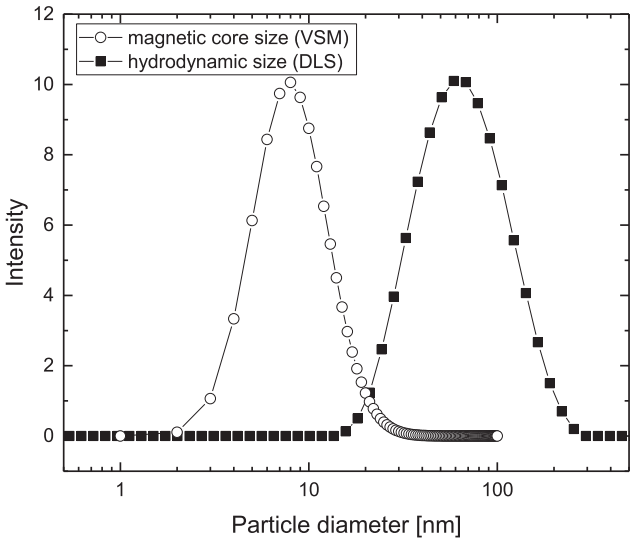

Fig. 2. Magnetic core size distribution obtained from magnetization curve and the hydrodynamic size of particles obtained from DLS measurement.

superparamagnetic behavior of the obtained magnetic nanoparticles. It also can be seen that the saturation magnetization is 0.0217 T (Fig. 1). To obtain information about the magnetic core size distribution (Fig. 2), the magnetization curve was fitted to the Langevin function [25]. The dominant magnetization comes from the particles with a magnetic core size of approximately 9.7 ± 0.1 nm. The coupling constant $\lambda \approx 1$ indicates a relatively week magnetic dipole interaction between particles. The hydrodynamic size distribution of nanoparticles was determined from DLS measurements using Malvern Zetasizer Nano ZS. The mean hydrodynamic diameter was approximately 58 ± 0.2 nm (Fig. 2). The nanoparticles diameter obtained from magnetic measurements is usually smaller than their hydrodynamic size since the magnetic measurements give only the size of the magnetic core whereas DLS method measures also the thickness of the other nonmagnetic layer or layers surrounding the magnetic grain.

2.2. Preparation and characterization of tissue-mimicking phantoms

For our studies we prepared tissue-mimicking materials based on agar powder – nontoxic substance obtained from red seaweeds. Agar phantom forms a thermo-reversible gel in an aqueous solution, and remains stable over a wide range of temperatures up to 353 K (80 °C) which is advantageous [26]. The acoustic parameters of agar phantoms such as speed of sound ~1540 m/s, density ~1.0 g/cm^3, and attenuation ~0.3–0.5 dB/cm·MHz, are very similar to those of human tissue [27]. For all of the hyperthermia measurements agar gel phantoms were prepared using agar powder characterized by the company HiMedia as a standard plate count agar (Standard Methods Agar M091-500G) and doped with magnetic nanoparticles (characterized in previous section). The prepared phantoms have a cylindrical shape with 3.0 cm diameter and height about 2.5 cm. The weight concentration of the agar in phantoms ϕ_A was 5% (w/w) and the concentration of the magnetic nanomaterial ϕ_M was approximately 0.35% (w/w), 0.64% (w/w) and 1% (w/w).

2.3. Measurement setup

During experiments on ultrasound, magnetic and sonomagnetic hyperthermia the measured sample, induction coil and ultrasound transducer were immersed in degassed and distilled water at room temperature. The phantom was first irradiated with either the focused ultrasound wave or exposed only to AC magnetic field. Then both heating sources were applied simultaneously. The focused single-

element ultrasound transducer made by Optel company was driven in continuous-wave mode with an operating frequency of 1 MHz. The acoustic power of the transducer was ranging from 0.3 to 1.9 W.

The compact EASYHEAT (Ambrell Corporation, United States) induction heating systems was used as a source of magnetic field. The induction heating setup consists of a high-frequency power supply that takes the input from the AC line mains. This power supply unit converts regular line frequency (50 Hz) to a high-frequency signal, typically operating between 150 and 400 kHz. This high-oscillating signal is then fed to a tank circuit that feeds the water-cooled induction heating coil. The high-frequency signal generates a high-frequency magnetic field inside the induction heating coil. The frequency of the alternating magnetic field is 356 kHz and the intensity ranges from 5.2 to 16.2 kA/m. The temperature in the phantom during all hyperthermia experiments was measured using a FLUOTEMP temperature sensor system (Photon Control Inc.). The temperature sensor consists of the optic fiber temperature probe (model FTP-NY2), the optic fiber cable, and the opto-electronic converter. Thermometer is connected to computer to register experimental data. The signal from the probe is unaffected by the magnetic field and other interferences. During experiments the optical fiber was centrally placed in the phantom about 0.5 cm below its surface, at the ultrasound focus and in the center of induction coil. In order to position the thermometer as close as possible to the focus of ultrasound beam, the phantom with optical fiber inside was mounted on a tri-axis positioning system (x, y, z). The ultrasound heating started after the focus point was found. Schematic illustration of the measurement setup is presented in Fig. 3. Ultrasound and magnetic hyperthermia experiments were conducted for three SPION concentrations of 0.35%, 0.64%, 1% (w/w) and various acoustic and magnetic field powers. Magneto-ultrasonic experiments were performed as a function of SPION concentration for 1 W of acoustic power and 10.7 kA/m magnetic field. The reason for the choice of 1 W-acoustic power was that it allowed us to achieve similar final temperatures of the samples in both procedures: ultrasonic and magnetic. Therefore any of these methods did not dominate the heating of the samples.

3. Results and discussion

3.1. Ultrasound hyperthermia

Ultrasound-based therapies play a fundamental role in the scientific research. Ultrasonic waves induce oscillation of materials in the ultrasound field. This mechanical oscillation is then converted into thermal energy, which increases the temperature in the treatment zone. Furthermore, focused ultrasound is a good technology for inducing hyperthermia because of its precise focus and ability to deposit energy in small area. First experiments of our work concerned the investigation of the effect of sonosensitizing nanoparticles presence on the temperature rise in the center of the ultrasound focal zone for different acoustic powers. The experimental results of recorded temperature changes versus time, for agar phantom doped with 1% concentration of SPION at different acoustic powers, are presented in Fig. 4a. It can be seen that the temperature increases with acoustic power. Because the focal zone is very small the observed temperature increase is rapid, in the first seconds of sonication, then it stabilizes and saturates. Since the ultrasound beam propagates through the phantom, some of its energy is deposited as heat. In normal circumstances, this heat would dissipate rapidly. The difference in rate of heating and cooling results as a local temperature rise [28]. Moreover, higher temperature rise is caused by the attenuation of bigger amount of ultrasound wave energy.

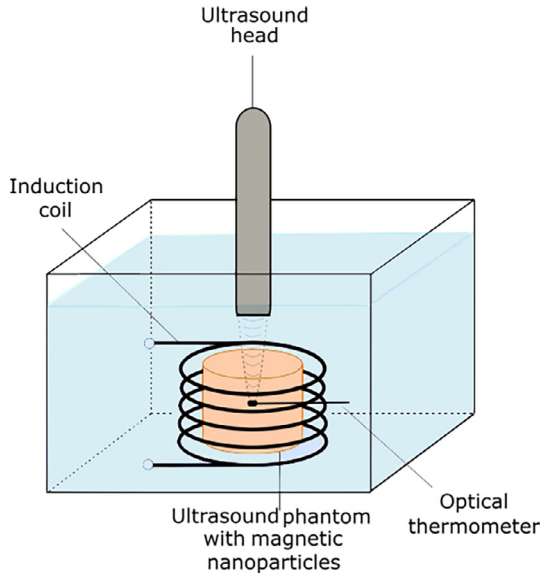

Fig. 3. Schematic illustration of the measurement setup.

The next goal of our research was to study the effect of magnetic nanoparticles concentration on the thermal effect of ultrasound hyperthermia. The temperature variations with time for various concentration of SPION during 1 W-ultrasound sonication at 1 MHz frequency are presented in Fig. 4b. We observed that bigger amount of nanoparticles leads to the additional attenuation of sound [15] and in consequence to the higher temperature increase. As it was described earlier the rapid temperature increase in the first seconds of ultrasound sonication and further temperature saturation also can be observed.

The effect of ultrasound sonication, in short, can be enhanced by sonosensitizers. Various nanometer sized particles have been successfully used as sonosensitizers to maximize the ultrasound action [29,30]. In our work we propose the use of magnetic nanoparticles modified with glycine because of their biocompatibility, nontoxicity, and common use in several medical applications [23,24]. Moreover, our results indicate their good sonosensitizing properties for the ultrasound hyperthermia treatments. Their presence in the tissue mimicking phantoms increases the rate of ultrasound heating.

3.2. Magnetic hyperthermia

Magnetic nanoparticles, despite being the source of additional attenuation in ultrasound hyperthermia, can also produce heat by themselves in the AC magnetic field. Magnetic hyperthermia is a promising non-invasive cancer medical therapy, which makes use of magnetic nanoparticles that generate heat. There are three mechanisms of magnetic heating: eddy currents, magnetic relaxation, and hysteresis losses. In the case of superparamagnetic magnetic particles the major heating mechanism is relaxation. Magnetic moment of magnetic nanoparticles tends to align with direction of magnetic field through the movement of the magnetic moment within a particle (Neel's relaxation) or the rotation of the whole particle (Brownian relaxation). The temperature variations with time for the phantom with 1% concentration of SPION for different values of the magnetic field strength during magnetic hyperthermia are presented in Fig. 5a. The higher the intensity of the magnetic field, the faster temperature rise was observed. For 5.2 kA/m the heating rate $\Delta T/\Delta t$ is about 0.012 °C/s and for 16.2 kA/m about 0.047 °C/s. The temperature increases achieved during those experiments are rather moderate. According to the literature [18,31] the confinement and immobilization of nanoparticles in a tissues or tissue-mimicking phantoms leads to the suppression of Brownian relaxation mechanism and in consequence causes a decrease in the heating efficacy.

The temperature variations with time during magnetic hyperthermia with the magnetic field strength of 10.7 kA/m for the phantoms with various concentration of SPION are presented in Fig. 5b. The higher amount of magnetic nanoparticles in phantom leads to the more effective heating. The heating effect was not observed in agar gel

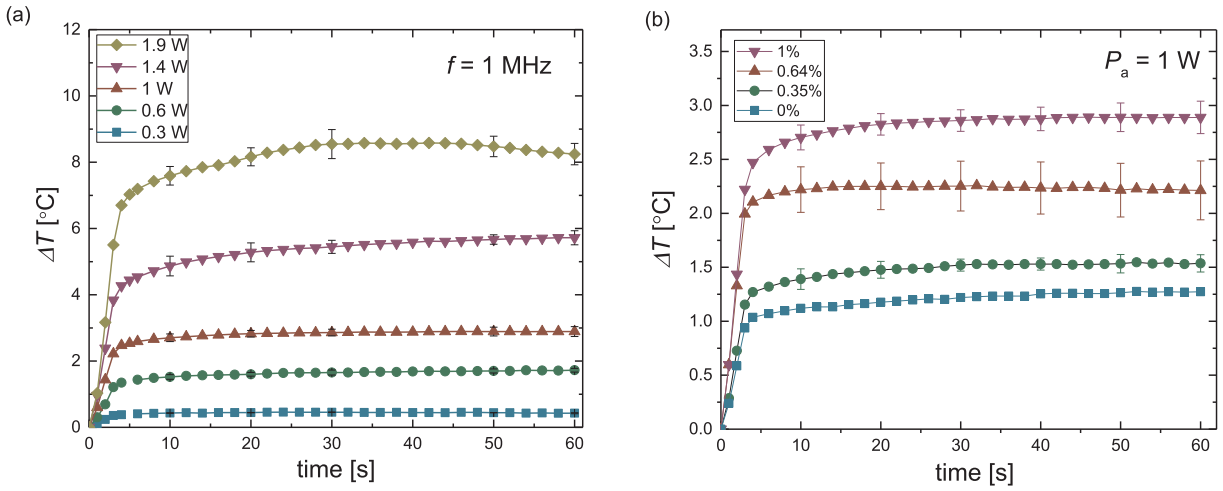

Fig. 4. (a) Ultrasound hyperthermia as a function of time and acoustic power for 1% concentration of SPION; (b) ultrasound hyperthermia as a function of time and SPION concentration for 1 W of acoustic power.

phantom without magnetite nanoparticles.

The results of our magnetic hyperthermia experiments have shown that the magnetic nanoparticles modified with glycine are good material for heat generation in AC magnetic field. In the presence of magnetic field they exhibit noticeable thermal effect. Their larger concentration in phantoms contributes to the higher increases of the magnetic hyperthermia efficacy.

3.3. Magneto-ultrasonic heating

The experiments described in the previous sections have shown that the prepared magnetic nanoparticles have the ability to act as direct source of heating (magnetic heating) and enhance the heating efficiency of the ultrasound by the increasing its absorption in the phantom. The most interesting, however, is the use of these two methods of heating together. The effect of sonomagnetic interaction was studied by applying simultaneously the magnetic field and ultrasound to the phantoms (Fig. 3). The results of sonomagnetic heating for different concentrations of SPION using the ultrasound at acoustic power of 1 W and the magnetic field of the strength equal to 10.7 kA/m are presented in Figs. 6–8 with the results of the single hyperthermia procedures (magnetic and ultrasound) shown for the comparison. The temperature achieved using sonomagnetic hyperthermia is higher in

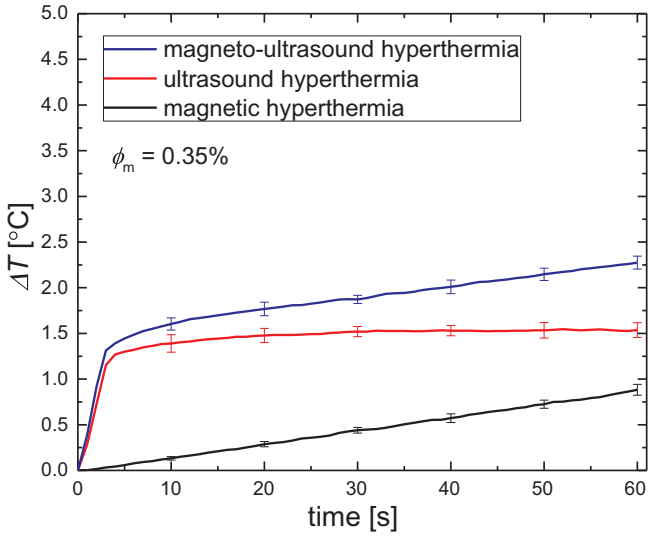

Fig. 6. Magnetic, ultrasound and magneto-ultrasound hyperthermia results for 0.35% concentration of SPION, for the ultrasound at acoustic power of 1 W and the strength of magnetic field of 10.7 kA/m magnetic field.

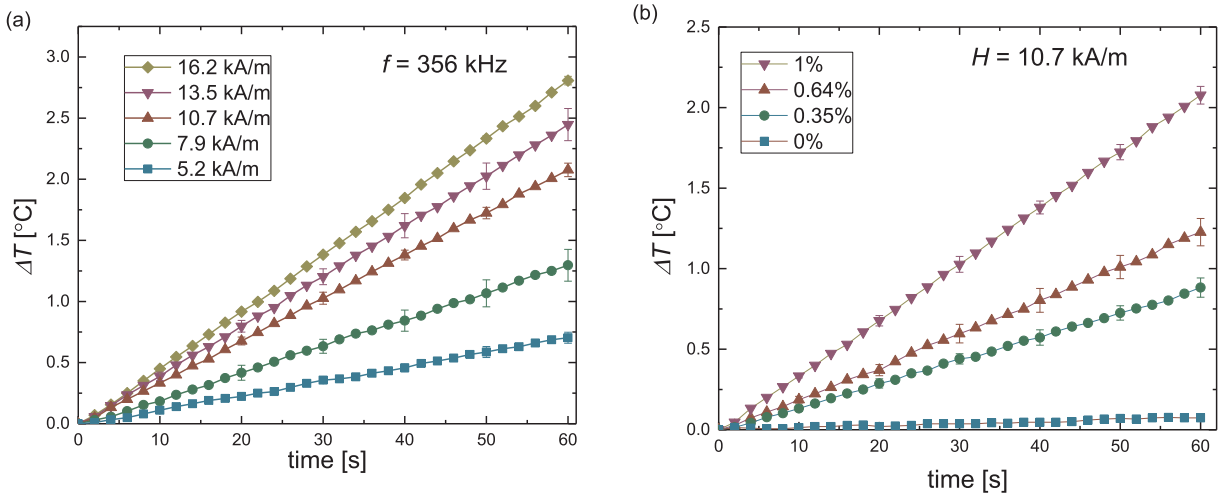

Fig. 5. (a) Magnetic hyperthermia as a function of time and magnetic field strength for 1% concentration of SPION; (b) magnetic hyperthermia as a function of time and SPION concentration for the magnetic field strength of 10.7 kA/m.

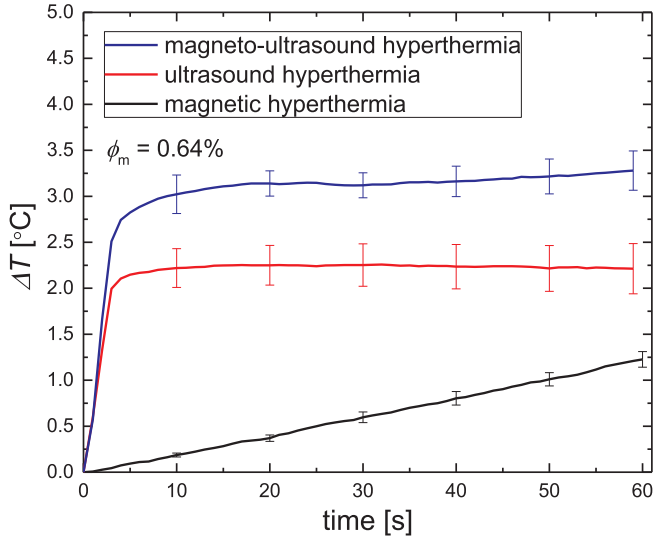

Fig. 7. The temperature increase in magnetic, ultrasound and magneto-ultrasound heating for 0.64% concentration of SPION. The acoustic power was 1 W and the strength of magnetic field was 10.7 kA/m.

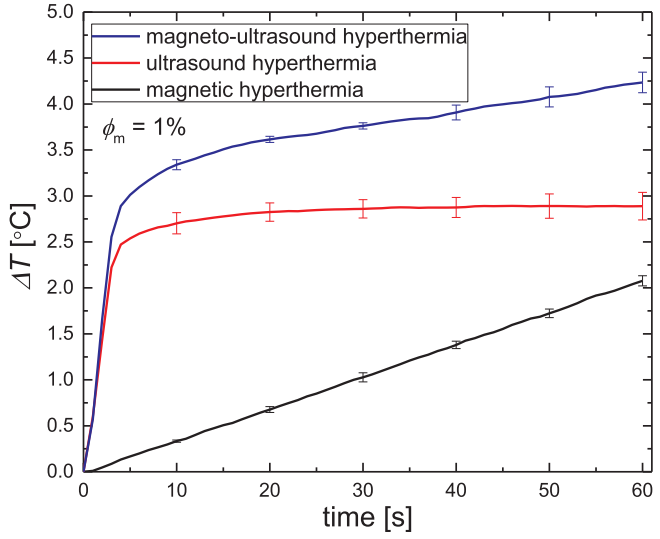

Fig. 8. The temperature increase during magnetic, ultrasound and magneto-ultrasound heating for 1% concentration of SPION. The acoustic power was 1 W and the strength of magnetic field was 10.7 kA/m.

comparison to the results obtained during ultrasound or magnetic hyperthermia alone. For example after 10 s in the AC magnetic field (10.7 kA/m) the temperature in the phantom of 1% concentration of SPION (Fig. 8) increased about 0.33 °C while after 10 s of ultrasound sonication (at acoustic power of 1 W) the temperature increased about 2.70 °C. On the other hand after 10 s of simultaneous actions of both heating modes the temperature increase was about 3.34 °C. It can clearly be seen that bimodal hyperthermia is more effective than single methods of hyperthermia. This innovative sonomagnetic hyperthermia will allow for a better control of the heating process and shorter exposures time what should lead to the more effective therapy.

Many experimental groups work to improve and modify the existing thermal procedures by combining them with other methods [1–4,6]. Bimodal sonomagnetic method proposed in this study seems to be very interesting and promising for further investigations and applications. The experimental results demonstrate that this combined method is characterized by a better heating ability than ultrasound or magnetic alone. We assume that the achieved improvement of heating rate in

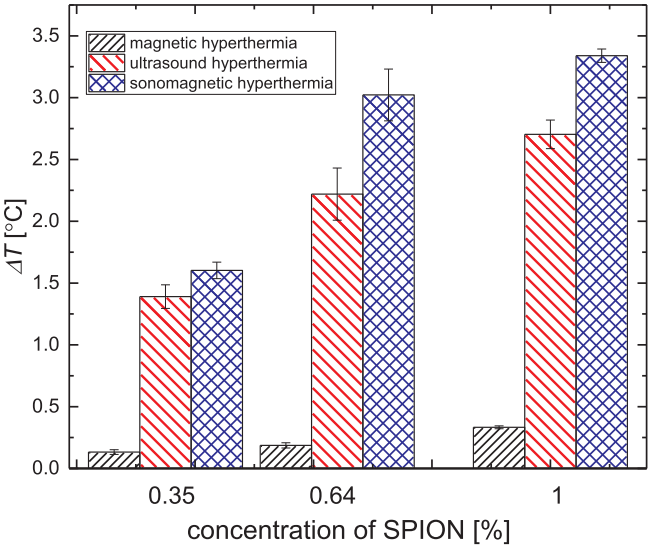

Fig. 9. The temperature increase during 10 s of magnetic, ultrasound and sonomagnetic heating for different concentrations of SPION. The ultrasound power was 1 W and the strength of magnetic field was 10.7 kA/m.

simultaneous interaction of ultrasounds and magnetic field probably results from the unlocking (in part) by ultrasonic wave the relaxation mechanism of the Brownian motions which are responsible for the heat generation in magnetic hyperthermia. In many studies the substantial effect of magnetic heating was observed in magnetic particle suspensions [32]. However, in gel matrix such as agar phantom these motions are blocked due to solid-like structure of gel. During sonomagnetic heating, the ultrasonic component significantly increases the temperature of phantom and the pores in agar expands similarly as during sonophoresis treatment [33]. This leaves more space for Brownian motions of nanoparticles during magnetic hyperthermia, which manifests in the observable additional temperature increase during sonomagnetic hyperthermia (Fig. 9).

4. Conclusion

The presented work involves the investigation of the effect of simultaneous interaction of ultrasounds and magnetic field with magnetic nanoparticles on the temperature increase in gel phantoms doped with magnetic nanoparticles. The effect of external physical stimulus, such as ultrasound and the AC magnetic fields, was assessed in vitro. We demonstrated that bimodal stimulation of nanoparticles provides a better heating efficiency. These two heating effects seem to be cumulative in nature. Simultaneous interaction of both thermal modes in the first seconds contribute to a higher temperature increase than either method alone or their sum. This sonomagnetic procedure provides a better heating efficiency and enables more precise control over the heating process. The obtained results suggest that magneto-ultrasonic approach to hyperthermia can also find the application in the treatment of the cancer as this method requires the lower SPION concentration that can reduce health risks. Summarizing, the coupling of magnetic and ultrasonic hyperthermia is promising heat therapy for tumor and can lead to the possibility of a new, innovative thermal method.

Acknowledgements

This work was partly supported by the grants 2015/17/B/ST7/03566 (OPUS) and 2017/27/N/ST7/00201 (PRELUDIUM) of the Polish National Science Centre and Slovak Research and Development Agency under the Contract No. APVV-15-0438.

References

[1] H. Chen, Y. Di, D. Chen, K. Madrid, M. Zhang, C. Tian, L. Tang, Y. Gu, Combined chemo- and photo-thermal therapy delivered by multifunctional theranostic gold nanorod-loaded microcapsules, Nanoscale 7 (2015) 8884–8897.

[2] R. Mendes, P. Pedrosa, J.C. Lima, A.R. Fernandes, P.V. Baptista, Photothermal enhancement of chemotherapy in breast cancer by visible irradiation of gold nanoparticles, Sci. Rep. 7 (2017) 10872.

[3] A. Espinosa, R. Di Corato, J. Kolosnjaj-Tabi, P. Flaud, T. Pellegrino, C. Wilhelm, Duality of iron oxide nanoparticles in cancer therapy: amplification of heating efficiency by magnetic hyperthermia and photothermal bimodal treatment, ACS Nano 10 (2016) 2436–2446.

[4] B. Xiao, L. Ma, D. Merlin, Nanoparticle-mediated co-delivery of chemotherapeutic agent and siRNA for combination cancer therapy, Expert Opin. Drug Deliv. 14 (2017) 65–73.

[5] J. Kim, B.C. Yung, W.J. Kim, X. Chen, Combination of nitric oxide and drug delivery systems: tools for overcoming drug resistance in chemotherapy, J. Control. Release 263 (2017) 223–230.

[6] H. Han, H. Lee, K. Kim, H. Kim, Effect of high intensity focused ultrasound (HIFU) in conjunction with a nanomedicines-microbubble complex for enhanced drug delivery, J. Control. Release 266 (2017) 75–86.

[7] A. Shakeri-Zadeh, S. Khoee, M.-B. Shiran, A.M. Sharifi, S. Khoei, Synergistic effects of magnetic drug targeting using a newly developed nanocapsule and tumor irradiation by ultrasound on CT26 tumors in BALB/c mice, J. Mater. Chem. B 3 (2015) 1879–1887.

[8] N. Frazier, H. Ghandehari, Hyperthermia approaches for enhanced delivery of nanomedicines to solid tumors, Biotechnol. Bioeng. 112 (2015) 1967–1983.

[9] A. de Leon, R. Perera, P. Nittayacharn, M. Cooley, O. Jung, A.A. Exner, Ultrasound contrast agents and delivery systems in cancer detection and therapy, Adv. Cancer Res. (2018).

[10] D.L. Miller, N.B. Smith, M.R. Bailey, Overview of therapeutic ultrasound applications and safety considerations, J. Ultrasound Med. 31 (2012) 623–634.

[11] S.A.R. Dibaji, M.F. Al-Rjoub, M.R. Myers, R.K. Banerjee, Enhanced heat transfer and thermal dose using magnetic nanoparticles during HIFU thermal ablation – an in vitro study, J. Nanotechnol. Eng. Med. 4 (2014) 040902.

[12] G.-Y. Wan, Y. Liu, B.-W. Chen, Y.-Y. Liu, Y.-S. Wang, N. Zhang, Recent advances of sonodynamic therapy in cancer treatment, Cancer Biol. Med. 13 (2016) 325–338.

[13] X. Qian, X. Han, Y. Chen, Insights into the unique functionality of inorganic micro/nanoparticles for versatile ultrasound theranostics, Biomaterials 142 (2017) 13–30.

[14] Y. Sun, Y. Zheng, H. Ran, Y. Zhou, H. Shen, Y. Chen, H. Chen, T.M. Krupka, A. Li, P. Li, Z. Wang, Z. Wang, Superparamagnetic PLGA-iron oxide microcapsules for dual-modality US/MR imaging and high intensity focused US breast cancer ablation, Biomaterials 33 (2012) 5854–5864.

[15] K. Kaczmarek, T. Hornowski, M. Kubovčíková, M. Timko, M. Koralewski, A. Józefczak, Heating induced by therapeutic ultrasound in the presence of magnetic nanoparticles, ACS Appl. Mater. Interfaces 10 (2018) 11554–11564.

[16] A. Józefczak, B. Leszczyński, A. Skumiel, T. Hornowski, A comparison between acoustic properties and heat effects in biogenic (magnetosomes) and abiotic magnetite nanoparticle suspensions, J. Magn. Magn. Mater. 407 (2016) 92–100.

[17] S. Dutz, R. Hergt, Magnetic particle hyperthermia—a promising tumour therapy? Nanotechnology 25 (2014) 452001.

[18] A. Józefczak, K. Kaczmarek, T. Hornowski, M. Kubovčíková, Z. Rozynek, M. Timko, A. Skumiel, Magnetic nanoparticles for enhancing the effectiveness of ultrasonic hyperthermia, Appl. Phys. Lett. 108 (2016) 263701.

[19] V. Zavisova, M. Koneracka, J. Kovac, M. Kubovcikova, I. Antal, P. Kopcansky, M. Bednarikova, M. Muckova, The cytotoxicity of iron oxide nanoparticles with different modifications evaluated in vitro, J. Magn. Magn. Mater. 380 (2015) 85–89.

[20] I. Khmara, M. Koneracka, M. Kubovcikova, V. Zavisova, I. Antal, K. Csach, P. Kopcansky, I. Vidlickova, L. Csaderova, S. Pastorekova, M. Zatovicova, Preparation of poly-L-lysine functionalized magnetic nanoparticles and their influence on viability of cancer cells, J. Magn. Magn. Mater. 427 (2017) 114–121.

[21] I. Antal, M. Koneracka, M. Kubovcikova, V. Zavisova, I. Khmara, D. Lucanska, L. Jelenska, I. Vidlickova, M. Zatovicova, S. Pastorekova, N. Bugarova, M. Micusik, M. Omastova, P. Kopcansky, d, l-lysine functionalized Fe_3O_4 nanoparticles for detection of cancer cells, Colloids Surf. B 163 (2018) 236–245.

[22] A. Bee, R. Massart, S. Neveu, Synthesis of very fine maghemite particles, J. Magn. Magn. Mater. 149 (1995) 6–9.

[23] N.C. Feitozaa, T.D. Gonçalves, J.J. Mesquita, J.S. Menegucci, M.-K.M.S. Santos, J.A. Chaker, R.B. Cunha, A.M.M. Medeiros, J.C. Rubim, M.H. Sousa, Fabrication of glycine-functionalized maghemite nanoparticles for magnetic removal of copper from wastewater, J. Hazard. Mater. 264 (2014) 153–160.

[24] K.C. Barick, P.A. Hassan, Glycine passivated Fe_3O_4 nanoparticles for thermal therapy, J. Colloid Interface Sci. 369 (2012) 96–102.

[25] Z. Rozynek, A. Józefczak, K.D. Knudsen, A. Skumiel, T. Hornowski, O. Fossum, M. Timko, P. Kopčanský, M. Koneracká, Structuring from nanoparticles in oil-based ferrofluids, Eur. Phys. J. E 34 (2011) 28.

[26] A. Dabbagh, B.J.J. Abdullah, C. Ramasindarum, N.H. Abu Kasim, Tissue-mimicking gel phantoms for thermal therapy studies, Ultrason. Imaging 36 (2014) 291–316.

[27] T.D. Mast, Empirical relationships between acoustic parameters in human soft tissues, Acoust. Res. Lett. Online 1 (2000) 37–42.

[28] D. Cranston, A review of high intensity focused ultrasound in relation to the treatment of renal tumours and other malignancies, Ultrason. Sonochem. 27 (2015) 654–658.

[29] A.P. Sviridov, V.G. Andreev, E.M. Ivanova, L.A. Osminkina, K.P. Tamarov, V.Y. Timoshenko, Porous silicon nanoparticles as sensitizers for ultrasonic hyperthermia, Appl. Phys. Lett. 103 (2013) 193110.

[30] S.B. Devarakonda, M.R. Myers, M. Lanier, C. Dumoulin, R.K. Banerjee, Assessment of gold nanoparticle-mediated-enhanced hyperthermia using MR-guided high-intensity focused ultrasound ablation procedure, Nano Lett. 17 (2017) 2532–2538.

[31] U. Engelmann, E.M. Buhl, M. Baumann, T. Schmitz-Rode, I. Slabu, Agglomeration of magnetic nanoparticles and its effects on magnetic hyperthermia, CDBME 3 (2017) 457–460.

[32] M. Timko, M. Molcan, A. Hashim, A. Skumiel, M. Müller, H. Gojzewski, A. Józefczak, J. Kovac, M. Rajnak, M. Makowski, P. Kopčanský, Hyperthermic effect in suspension of magnetosomes prepared by various methods, IEEE Trans. Magn. (2013) 250–254.

[33] J. Narayanan, J.-Y. Xiong, X.-Y. Liu, Determination of agarose gel pore size: absorbance measurements vis a vis other techniques, J. Phys. Conf. Ser. 28 (2006) 83.